CHALMERS

Nanocrystalline Cellulose as a Drug Carrier of Cyanine Dyes to DNA

Bachelor Science Thesis

Simon Jademyr

Department of Chemistry and Chemical Engineering
CHALMERS UNIVERSITY OF TECHNOLOGY
Gothenburg, Sweden 2016

Nanocrystalline Cellulose as a Drug Carrier of Cyanine Dyes to DNA

SIMON JADEMYR

Supervisor: Gunnar Westman

Department of Chemistry and Chemical Engineering

Division of Organic Chemistry

CHALMERS UNIVERSITY OF TECHNOLOGY

Göteborg, Sweden 2016

Nanocrystalline Cellulose as a Drug Carrier of Cyanine Dyes to DNA

SIMON JADEMYR

Department of Chemistry and Chemical Engineering

Division of Organic Chemistry

Chalmers University of Technology

SE-412 96 Göteborg

Sweden

Telephone +46 (0)73 075 3909

Nanocrystalline Cellulose as a Drug Carrier of Cyanine Dyes to DNA

SIMON JADEMYR

Department of Chemistry and Chemical Engineering

Chalmers University of Technology

ABSTRACT

The objectives of the project was to study the behavior of the cyanine dyes TO and BO together with nanocrystalline cellulose and DNA by using spectroscopic analysis. The cyanine dyes were synthesized and analyzed with NMR and the nanocrystalline cellulose were prepared by sulfuric acid hydrolysis on microcrystalline cellulose and then analyzed by FT-IR, X-Ray diffraction and atomic force microscopy.

The possibility of transferring the cyanine dyes from the surface of nanocrystalline cellulose to DNA in aqueous solutions was examined and the results confirmed that it is indeed possible, both for TO and for BO.

Additionally, aggregation of the cyanine dyes TO and BO were examined both by themselves and also combined with nanocrystalline cellulose. The results showed that TO forms dimers with itself and combined with nanocrystalline cellulose H-aggregates are formed. At the measured concentrations no signs of aggregation were detected for BO.

A few preliminary tests investigating the possibility of using the cyanine dyes TO and BO for quantification of sulfate groups on nanocrystalline cellulose were also performed and it was concluded that it should be possible to use these cyanine dyes for developing a quantification method for sulfate groups on nanocrystalline cellulose.

Keywords: Nanocrystalline cellulose, cyanine dyes, H-aggregate, drug carrier, DNA, intercalation, spectroscopy, fluorescence, sulfate groups and quantification.

SAMMANFATTNING

Målen med projektet var att studera beteendet hos cyaninfärgämnena TO och BO tillsammans med nanokristallin cellulosa och DNA med hjälp av spektroskopiska analyser. Cyaninfärgämnena syntetiseras och analyserades med NMR och den nanokristallina cellulosan bereddes genom svavelsyrahydrolys på mikrokristallin cellulosa och analyserades därefter med FT-IR, röntgendiffraktion och atomkraftsmikroskopi.

Möjligheten att överföra cyaninfärgämnen från ytan på nanokristallin cellulosa till DNA i vattenlösning undersöktes och resultaten visade att det är möjligt både för TO och för BO.

Aggregering av cyaninfärgämnena TO och BO undersöktes både enskilt och tillsammans med nanokristallin cellulosa. Resultaten visade att TO bildar dimerer med sig själv, och att den tillsammans med nanokristallin cellulosa bildar H-aggregat. Vid de uppmätta koncentrationerna detekterades ingen aggregatbildning för BO.

Dessutom utfördes några preliminära tester för att undersöka om det är möjligt att använda cyaninfärgämnena TO och BO för att kvantifera sulfatgrupper på nanokristallin cellulosa. Mätningarna visade att det borde vara möjligt att använda dessa cyaninfärgämnen för att utveckla en metod för kvantifiering av sulfatgrupper på nanokristallin cellulosa.

ABBREVATIONS

CNC	Nanocrystalline cellulose
MCC	Microcrystalline cellulose
TO	Thiazole orange
BO	1-Methyl-4-[(3-methyl-1,3-benzothiazol-2(3H)-yliden)methyl]pyridinium
AFM	Atomic force microscopy
XRD	X-Ray diffraction
MWCO	Molecular weight cut-off

TABLE OF CONTENTS

1. INTRODUCTION

1.1 Background

Conventional chemotherapeutic antitumour drugs suffer from major drawbacks such as adverse effects on normal cells and resistance against the drug from the cell itself, which may lead to the necessity of administering several different drugs with complementary action. To overcome these drawbacks of current chemotherapy methods, there is an increasing need of developing new antitumour drugs with high selectivity regarding healthy and tumour cells. [1]

One potential type of compounds that has shown to inhibit growth of tumour cells [1] as well as selectively binding to DNA are cyanines. [2][3] Because of their unique optical properties and tendency to form aggregates with themselves or other compounds [4] they may at the same time be used as tools to study and visualize the DNA. [5][6]

In order to achieve the desired effects of antitumour drugs, they must first be delivered to the affected cells. One promising group of drug carriers that have gained a lot of interest are nanoparticles. Because of their small size they can cross cell membranes and reach the cell nucleus as well as other cellular compartments. It has however been reported that nanoparticles themselves may be hazardous which have led to an increasing desire to find safe non-toxic nanomaterials that can function as drug carriers. [7]

One material that matches these demands is nanocrystalline cellulose (CNC). It is a non-toxic, renewable and environmentally friendly nano material. It is traditionally made by acidic hydrolysis of cellulose, a preparation that will attach different quantities of charged functional groups such as sulfonate on the surface of the nanocrystals. [8] Because of the charged surface, nanocrystalline cellulose could potentially bind to a vast range of different pharmaceuticals or other compounds.

In this work the use of CNC as a drug carrier to DNA has been investigated. It was found that CNC could be used as a shuttle for cyanine dyes to DNA.

1.2 Objectives

The main aim of this study was to examine if the cyanine dyes TO and BO could be transferred from CNC to DNA, and also to investigate if the cyanine dyes form aggregates with themselves or combined with CNC.

Preliminary studies at the department has shown that the fluorescence of sulfonate groups on CNC can be reduced by the addition of the cyanine dye TO. Thus the secondary aim of the study was to further examine if TO have this effect on CNC, and also to test the same concept with another cyanine BO, as well as with other structurally simpler aromatic amines, and evaluate if any of these compounds could be used as a mean to quantify the amount of sulfonate groups on CNC.

2. THEORY

2.1 Nanocrystalline Cellulose

Cellulose, the world's most abundant renewable polymer consists of long linear chains of d-glucopyranose units linked together with beta-glycosidic bonds (Figure 1). The repeating d-glucopyranose units all have three hydroxyl groups attached to them which gives cellulose the ability to form hydrogen bonds. The hydroxyl groups contributes to many of the physical characteristic properties of cellulose such as its high functionality, hydrophilicty and crystalline packing. [8][9]

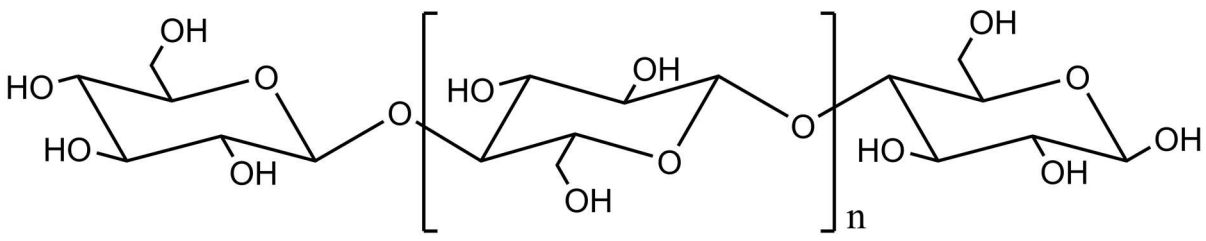

Figure 1. *Cellulose with its d-glucopyranose units forming a polymer.*

Since cellulose is a polymer it contains highly oriented crystalline regions as well as less ordered amorphous regions. [9] These crystalline regions can be isolated as crystallites commonly referred to as nanocrystalline cellulose (CNC). CNC generally consists of small rod-like crystals with a length and diameter usually ranging between a few hundred nanometers and 10-20 nanometers respectively. CNC exhibit several advantages compared to ordinary cellulose such as a high surface area, small size, unique optical features, and stability in aqueous suspension. [8]

Isolation of CNC from cellulose fibers is traditionally achieved by treating it with an acid, this will cause hydrolysis of the cellulose chains and cleave some of the glycosidic bonds. The crystalline regions of the fiber have a higher resistance to acids than the amorphous regions, meaning that the hydrolysis will affect the amorphous regions at a higher extent, thus causing them to get cleaved at a higher rate than the crystalline parts (Figure 2). [8][9]

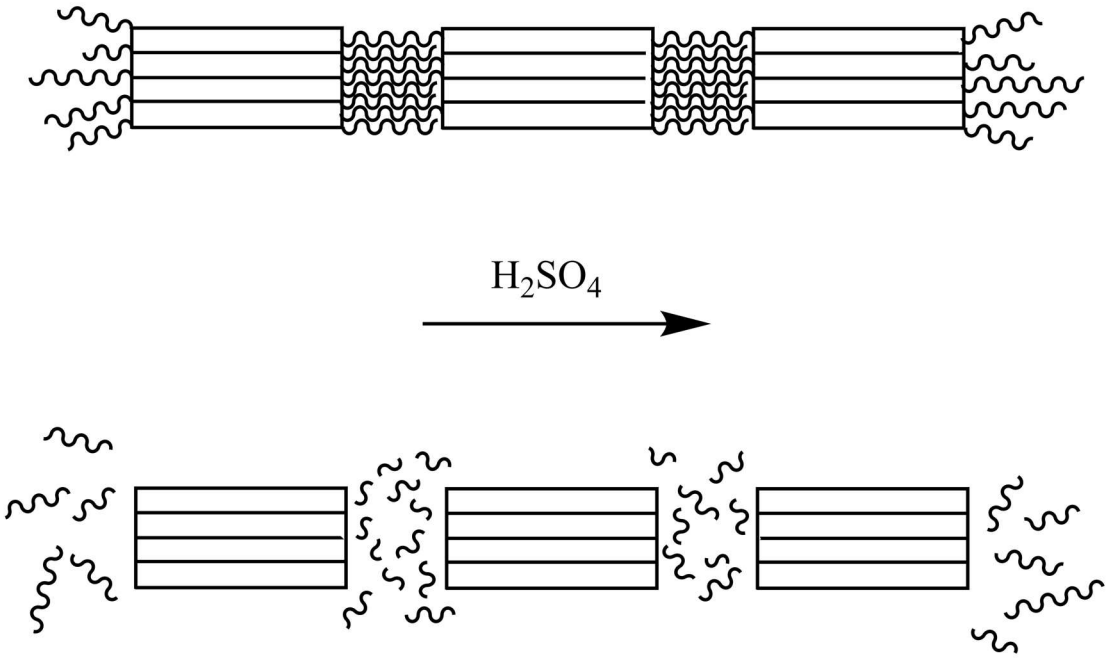

Figure 2. *Simplified schematic on how nanocrystalline cellulose is obtained by cleavage of the amorphous parts of the cellulose polymer by sulfuric acid hydrolysis. [8][10]*

Depending on the hydrolysis conditions such as temperature and reaction time, as well as the type of cellulose starting material, the produced CNC will receive various properties such as different dimensions, morphology and degree of crystallinity. [8][9]

Different types of acids used in the hydrolysis will give different functional groups on the CNC surface. For instance sulfuric acid will introduce sulfonate groups (Figure 3). [10] Conveniently the sulfonate groups will cause the cleaved amorphous cellulose to become water soluble while the CNC will remain insoluble which facilitates the isolation of the CNC. The introduced sulfate groups also enables the CNC to be readily dispersed and stabilized in aqueous solutions. [8]

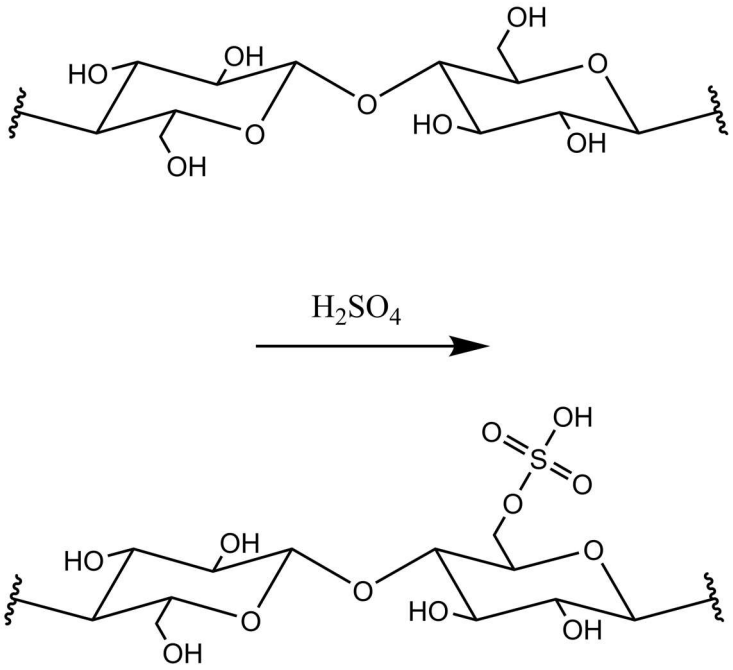

Figure 3. *Schematic showing how sulfonate groups attach to some of the hydroxyl groups on the cellulose chain during hydrolysis by sulfuric acid. [10]*

2.2 Cyanine Dyes

Cyanine dyes are a class of compounds that produces strong and well defined absorption bands in the visible UV spectra. They have been used extensively in a variety of different applications such as studying biological systems or as sensitizers in photographic films. [6] They are generally consisting of two nitrogen containing heterocyclic rings of which one of the nitrogens are positively charged (Figure 4). These heterocyclic rings are linked together by an odd number of methine groups that forms a conjugated chain of trans-oriented double

bonds between the nitrogens which causes the characteristic optical properties of the cyanine dyes. [6][11]

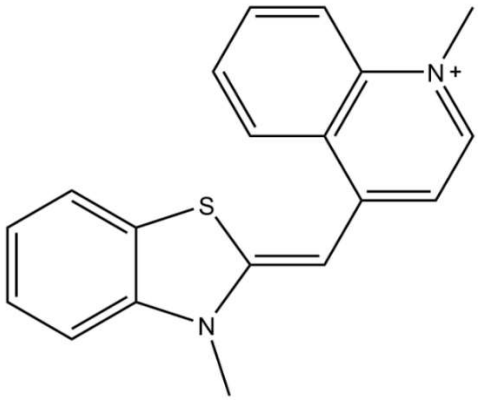

Figure 4. *Example of the molecular structure of a cyanine dye. The cyanine depicted is the commercially available thiazole orange (TO).*

2.2.1 Aggregation of Cyanine Dyes

Cyanine dyes have a tendency to form reversible non-covalently bonded aggregates in solutions. A few proposed mechanisms explaining this behavior has been made, such as van der Waals forces between the cyanine molecules, hydrophobic interactions, coordination with metal ions, or interactions with the solvent. It is known however that aggregation is facilitated by using water as a solvent, which is likely due to water having a high dielectric constant that reduces the repulsive effects of the positively charged cyanine molecules. [6][11]

The extent of formation of these aggregates does not only depend on solvent choice but a range of different factors such as molecular structures of the dyes, concentrations, temperature and pH. [6][11] Aggregation may also be promoted by adding certain polyelectrolytes such as polysulfonates or polyphosphates. [6][12]

The extent and type of aggregation is often easily monitored by simple absorption spectroscopy, this is possible because the aggregates cause significant electron delocalization over the aggregate structures, which causes the absorption band to dislocate relative to the monomeric non-aggregated cyanine dye. [11]

The simplest aggregate that can be formed is a dimer, its formation is favored by increased concentrations of cyanine. [13] This type of aggregation causes the absorption band to dislocate to a slightly lower wavelength relative to the monomer. [13][11]

When the dye molecules arrange themselves in a parallel face-to-face fashion the absorption band appears at lower wavelengths, this type of aggregation is referred to as an H-aggregate. The cyanines may also arrange themselves in a head-to-tail fashion which gives an absorption spectra where the band appears as a narrow high intensity peak at higher wavelengths, this is called a J-aggregate (Figure 5). [11][6]

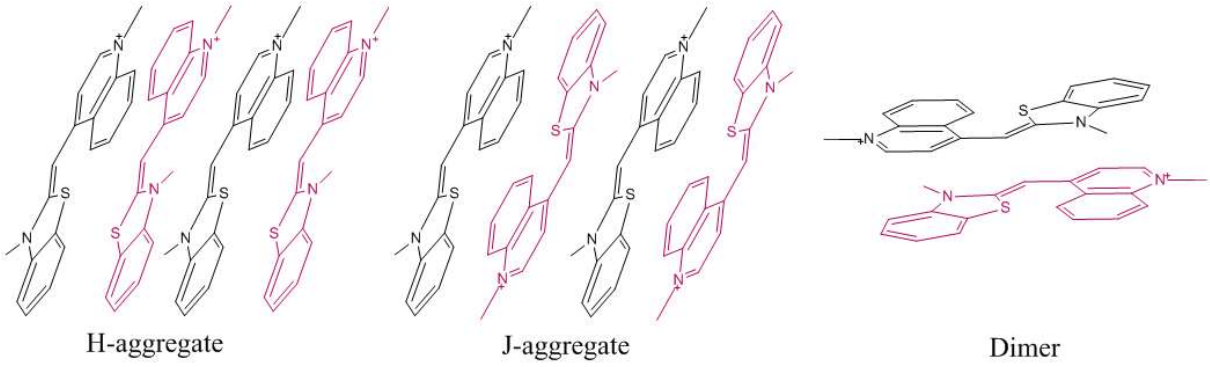

Figure 5. *Thiazole orange forming different types of aggregates with itself. [14]*

2.2.2 Cyanine Dyes and DNA

Many cyanine dyes are capable of interacting with DNA by insertion between the planar bases of DNA. This type of interaction is called intercalation. [15] Interestingly cyanines are often weakly- or non-fluorescent by themselves, but upon binding to DNA its fluorescence is greatly enhanced, a property that allows easy monitoring of cyanine and DNA bonding. [2] The high increase of fluorescence is believed to be caused by DNA hindering rotation and torsion around the methane bridge in the cyanine structure. [3] Thus when cyanine is irradiated with light, the absorbed energy that would normally cause movement of the molecule is forced to be emitted as light instead.

3. EXPERIMENTAL

3.1 Materials

3.1.1 Chemicals

Microcrystalline cellulose, Avicel® PH-101 from Sigma Aldrich
Sulfuric acid from Sigma Aldrich
DNA, calf thymus from Sigma Aldrich

3.1.2 Apparatus

Centrifuge, Heraeus Megafuge 40
Sonicator, Sonics Vibra Cell
FT-IR, Spectrum one from PerkinElmer instruments
XRD, D5000 from Siemens
AFM, NanoScope III from Digital instruments
UV-Vis, Cary 50 Bio from Varian Australia
Fluorescence, Cary Eclipse from Varian Australia

3.2 Methods

3.2.1 Preparation of CNC

With strong stirring 40 g of microcrystalline cellulose (MCC) were suspended in a solution of 64 % H_2SO_4 at 45°C. After two hours of stirring at 45°C the reaction were quenched by pouring it into 7 liters of deionized water.

The suspension were then centrifuged at 4300 rpm for 15 minutes and the water decanted. In order to remove any remaining acid the residual solids were then suspended in 2 liters of deionized water and placed in dialysis membranes (MWCO: 12-14000 g/mol). The membranes were then placed in a large container with deionized water. The water were changed regularly until the conductivity of the water was below 5 μS, this took several days.

After the dialysis was complete the suspension were subjected to sonication for 6x7 minutes at a 40 % amplitude in order to thoroughly disperse the particles in the suspension. By drying a pre-weighed sample of the obtained suspension in an infrared drying balance, the dry weight of CNC in the final product suspension were determined to be 1.42 %.

3.2.1.1 FT-IR analysis of CNC

In order to determine if the prepared CNC had obtained a higher degree of crystallinity compared to the MCC starting material, the CNC as well as the MCC were analyzed with FT-IR.

The FT-IR samples were prepared by grounding 2 mg of the dry materials together with 300 mg of potassium bromide into a fine powder. The powders were pressed into thin pellets under 8 tons of pressure. The pellets were then subjected to FT-IR analysis in the 4000-400 cm^{-1} range.

The crystallinity index of the samples were determined by taking the ratio of the band intensity at 1425 cm^{-1} and 900 cm^{-1}. [16]

3.2.1.2 XRD analysis of CNC

As a complement to the FT-IR analysis the MCC starting material and the prepared CNC was also subjected to X-ray diffraction analysis. The dried and finely grounded samples were analyzed in the X-ray diffractometer with 2θ-range 10-60°.

The crystallinity of the samples were calculated according to the Peak height method, where the height of the crystalline peak is compared to the height of the amorphous minimum. [17][18]

3.2.1.3 AFM analysis of CNC

The prepared CNC were also analysed with atomic force microscopy (AFM) in order to determine if the hydrolysis had succeeded and nanocrystals were present. A suspension containing 0.01% CNC and 7 μM TO were subjected to ultrasonification for 15 minutes then one drop of the suspension were placed on a mica plate and allowed to air dry. This sample was then analyzed by AFM.

3.2.2 Synthesis of Cyanine Dyes

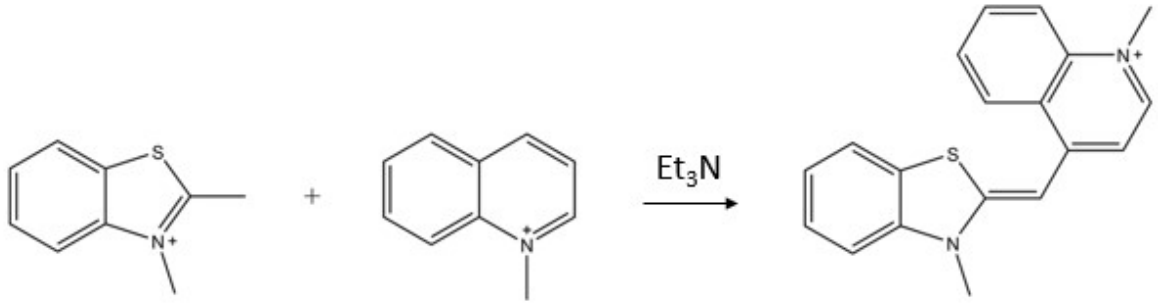

Figure 6. Schematic of the synthesis of TO.

1-Methyl-4-[(3-methyl-2(3*H*)-benzothiazolylidene)methyl]quinolinium tosylate (TO)
2,3-Dimethyl-1,3-benzothiazol-3-ium tosylate (671 mg, 2 mmol) and 1-Methylquinolinium tosylate (631 mg, 2 mmol) were suspended in 10 ml dichloromethane. Triethylamine (600 μq, 4.3 mmol) were added which caused the solids to dissolve and the mixture became deep red. After stirring 20 h at room temperature, 4 ml ethyl acetate were added and stirred for 15 min. The mixture were then filtered and the red solids were washed with small portions of ethyl acetate. The solids were then suspended in 8 ml ethyl acetate and heated for a few minutes. After cooling to room temperature the suspension were filtered and the solids were washed with small portions of ethyl acetate to give thiazole orange (255 mg, 27%). ^{1}H NMR (CD_3OD): δ 2.34 (3H, s), 3.98 (3H, s), 4.17 (3H, s), 6.91 (1H, s), 7.20 (2H, d, J=7.9), 7.40 (1H, t, J=15.2), 7.45 (1H, d, J=7.2), 7.59 (1H, t, J=15.2), 7.64 (1H, d, J=8.4), 7.69 (2H, d, J=8.2), 7.76 (1H, t, J=15.0), 7.87 (1H, d, J=8.0), 7.98 (1H, t, J=15.6), 8.01 (1H, d, J=6.8), 8.37 (1H, d, J=7.2), 8.65 (1H, d, J=8.4). ^{13}C NMR (CD_3OD): δ 19.85, 32.57, 41.73, 46.93, 48.21, 87.62, 108.29, 112.31, 117.52, 122.28, 124.41, 124.94, 125.64, 126.89, 128.06, 128.31, 133.08, 144.42.

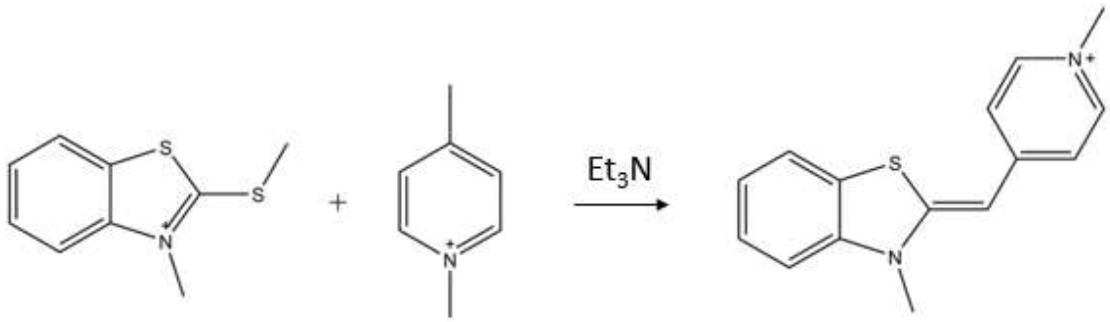

Figure 7. Schematic of the synthesis of BO.

(Z)-1-methyl-4-((3-methylbenzo[d]thiazol-2(3H)-ylidene)methyl)pyridin-1-ium 4-methylbenzenesulfonate (BO) 3-methyl-2-(methylthio)benzo[d]thiazol-3-ium benzenesulfonate (342 mg, 1.2 mmol) and 1,4-dimethylpyridin-1-ium benzenesulfonate (747 mg, 2 mmol) were suspended in 10 ml dichloromethane. Triethylamine (0.6 ml, 4.3 mmol) were then added which caused the suspension to become yellow. The mixture were then stirred for 20 h at room temperature. Ethyl acetate was added and the suspension were allowed to stir for an additional 15 minutes. The mixture were then filtered and washed with small portions of ethyl acetate. The solids were then heated with 10 ml of ethyl acetate and then cooled down and filtered to give BO (373 mg, 71%). ^{1}H NMR (CD_3OD): δ 2.35 (3H, s), 3.73 (3H), 3.99 (3H, s), 6.14 (1H, s), 7.21 (2H, d, J=8.0), 7.30 (1H, t, J=14.8), 7.40 (2H, d, J=7.2), 7.48 (1H, d, J=8.8), 7.52 (1H, t, J=15.6), 7.69 (2H, d, J=11.2), 7.76 (1H, d, J=8.0), 8.08 (2H, d, J=7.6). ^{13}C NMR (CD_3OD): δ 19.93, 31.8, 44.1, 46.92, 48.21, 89.13, 111.42, 118.67, 121.87, 123.57, 125.44, 127.75, 128.42, 141.38.

3.2.3 Preparation of Spectroscopy Samples

All samples subjected to absorption and emission spectroscopy were mixed and diluted directly in a quartz cuvette. Dilutions were performed with a 25 mM disodium phosphate buffer solution so that the final volume filled up the whole cuvette. The cuvette were then shaken for 2 minutes in order to enable aggregate formation. All the measurements were performed at room temperature.

4. RESULTS AND DISCUSSION

4.1 CNC characterization

4.1.1 FT-IR

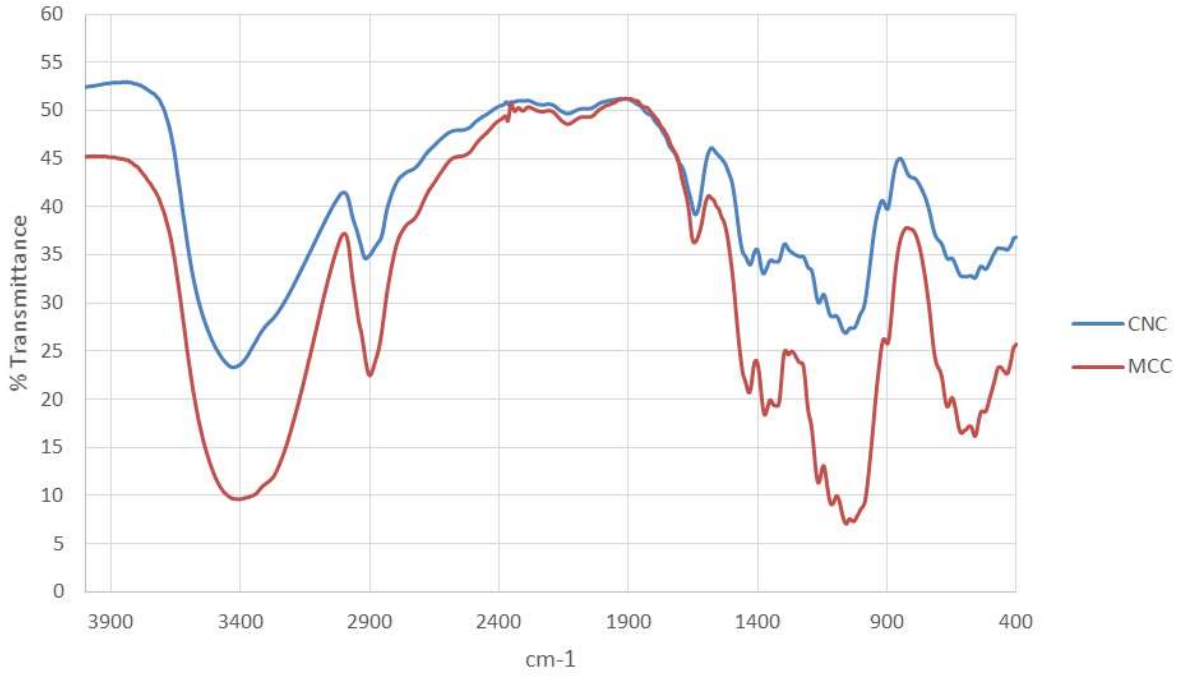

Figure 8. *IR spectra of CNC prepared by hydrolysis using sulfuric acid and the starting material MCC.*

FT-IR analysis (Figure 8) of the prepared CNC indicated that it was more crystalline than the starting material MCC. Crystallinity index were calculated as described in chapter 3.2.1.1 to 0.86 for CNC and 0.83 for MCC, which indicates that the prepared CNC were slightly more crystalline than the starting material MCC. The peak for the CNC curve at 3400 cm^{-1} were both slightly sharper and not as deep as the MCC, both of these data suggests a higher crystallinity for the prepared CNC. [16][19]

4.1.2 X-Ray Diffraction

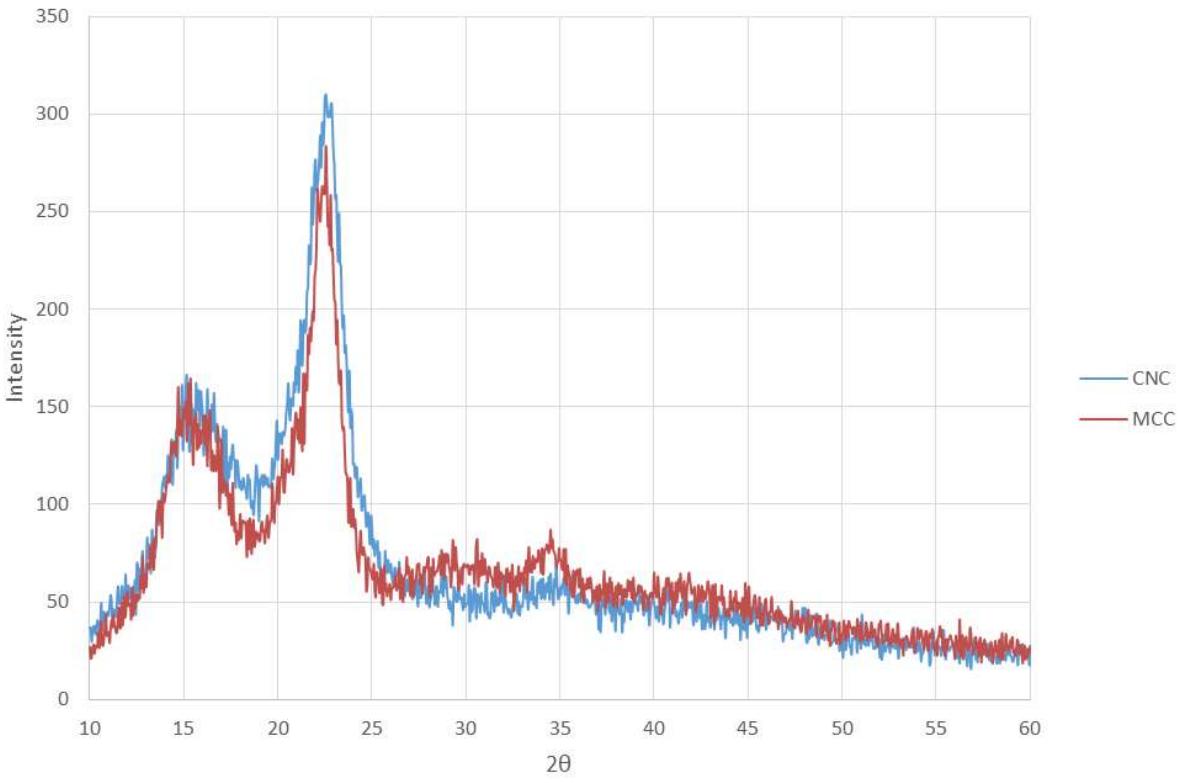

Figure 9. *X-ray diffraction peaks of CNC prepared by hydrolysis using sulfuric acid and the starting material MCC.*

The data obtained from the XRD analysis (Figure 9) shows slightly broader peaks for the CNC compared to the MCC, which suggests a higher crystallinity for CNC compared to MCC. [20]

According to the Peak height method [17][18] the crystallinity for CNC was determined to be 70.3% and for MCC 71.7%. Even though this method is not an accurate method to determine crystallinity, its reported to be adequate for comparing the crystallinity of two different materials. [18] If the prepared CNC is indeed of higher crystallinity than MCC as the FT-IR analysis suggests (Chapter 4.1.1) one possible source of error which might explain the contradicting results with XRD is that the CNC sample that were analyzed was not as finely powdered as the MCC.

4.1.3 AFM

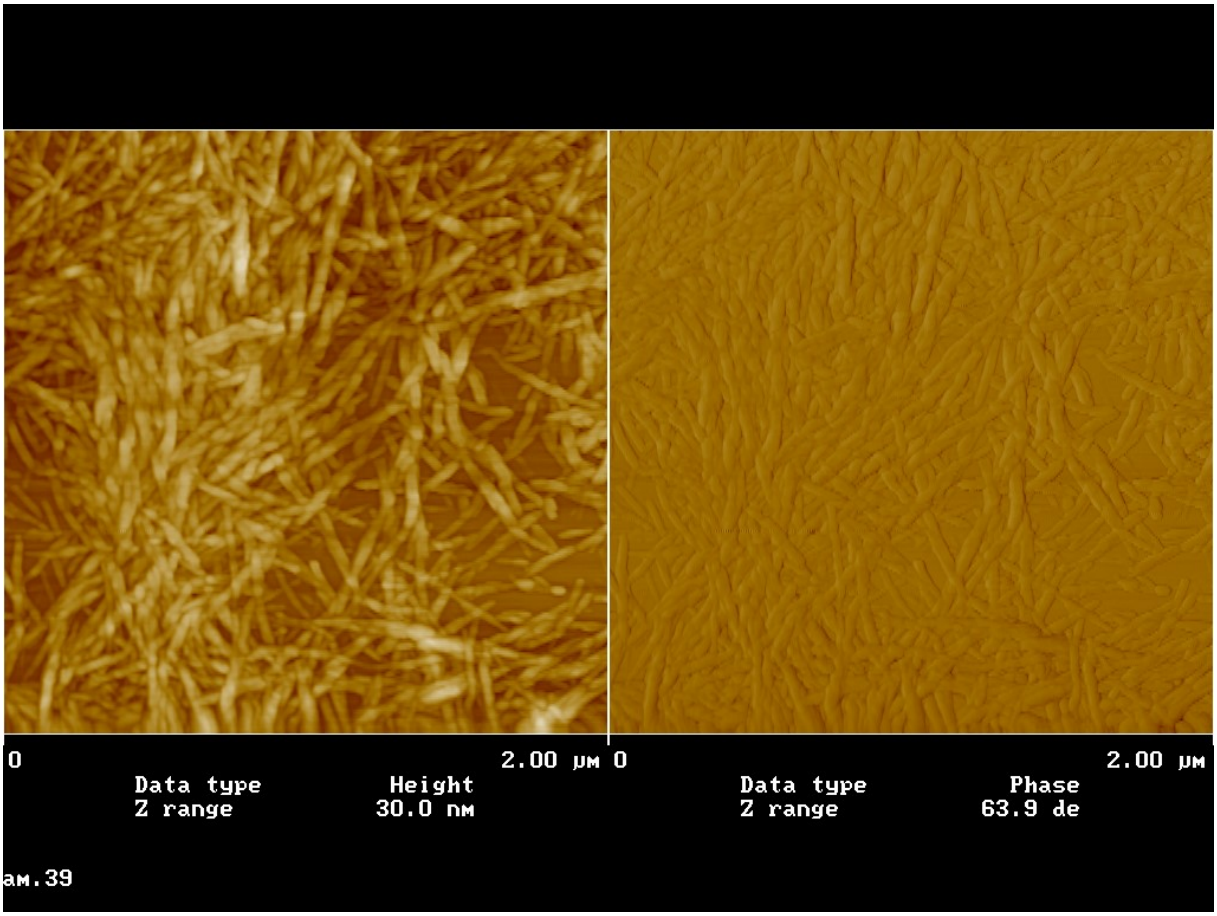

Figure 10. *AFM picture of a dried suspension containing 0.01 % CNC and 7 µM TO.*

AFM analysis of the dried CNC and TO suspension (Figure 10) showed tightly placed rod-like objects that indicates presence of nanocrystalline cellulose. The concentration used were slightly too high why the exact dimension of the crystallites were difficult to determine, they do however look slightly larger than what is normal which might have been caused by too mild hydrolysis conditions. Overall however the preparation of CNC from MCC were considered a success.

4.2 Cyanine Dye Aggregation

4.2.1 TO

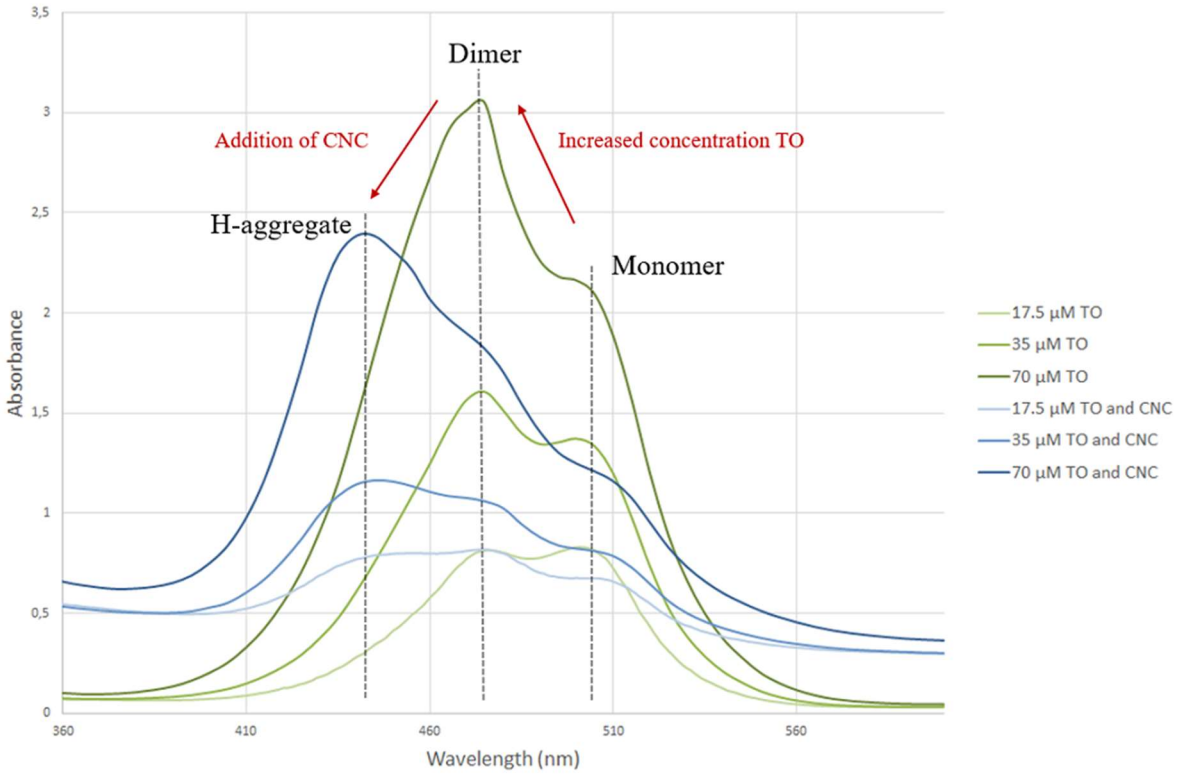

Figure 11. *Absorption spectra of different concentrations TO and 0.1 % CNC. All samples contained 25 mM of disodium phosphate buffer.*

The absorption bands (Figure 11) reveals three different peaks. Where the broader peak at around 440 nm indicates H-aggregation and the peaks at 470 and 500 nm indicates dimer and monomer aggregation respectively. It can be seen in the spectra that addition of CNC to TO causes the band peaks to be displaced to lower wavelengths, this is an indication that H-aggregates are formed when TO is combined with CNC. The spectra also shows that TO in lower concentrations are present mostly in its monomer form but as the concentration of TO is increased it starts forming dimer aggregates with itself.

The tendency of TO to form dimers with itself might partly be caused by its hydrophobicity, in polar solutions such as water this would cause the hydrophobic TO molecules to bundle together. It is also possible that the aggregation between CNC and TO is further promoted by the charged anionic surface of the CNC and the cationic TO causing the cyanine molecules to be forced close enough to each other to start forming aggregates

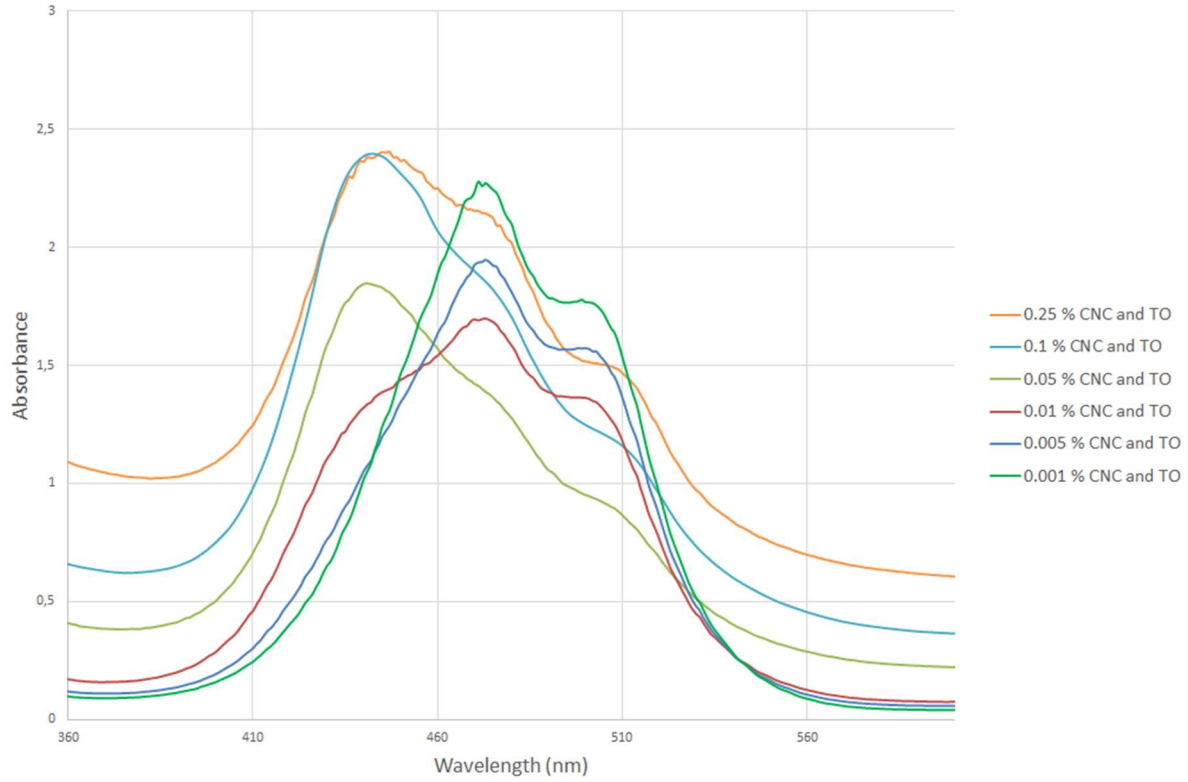

Figure 12. *Absorption spectra of different concentrations of CNC and 70 µM TO. All samples contained 25 mM of disodium phosphate buffer.*

In order to determine how the proportions of CNC to TO affected the formation of H-aggregates, the concentration of CNC was varied to a fixed concentration of TO. The results (Figure 12) shows that when the concentration of CNC is too low no H-aggregates are formed and the TO stays unaffected in its dimeric and monomeric forms.

As the concentration of CNC is increased however, the band starts to shift towards H-aggregation, and at 0.1 % CNC to 70 µM TO the dimer and monomer is only very slightly present. Interestingly, when the concentration of CNC is increased even further to 0.25 %

there is no more band shifting to H-aggregate but instead the dimer and monomer aggregates starts regenerating. It is possible that this occurs because increased CNC concentration might lead to such tight packaging between the CNC polymers that there is no room left for TO to attach to the CNC surface, thus causing the H-aggregates to disintegrate and the dimer and monomer aggregates to start regenerating.

4.2.2 BO

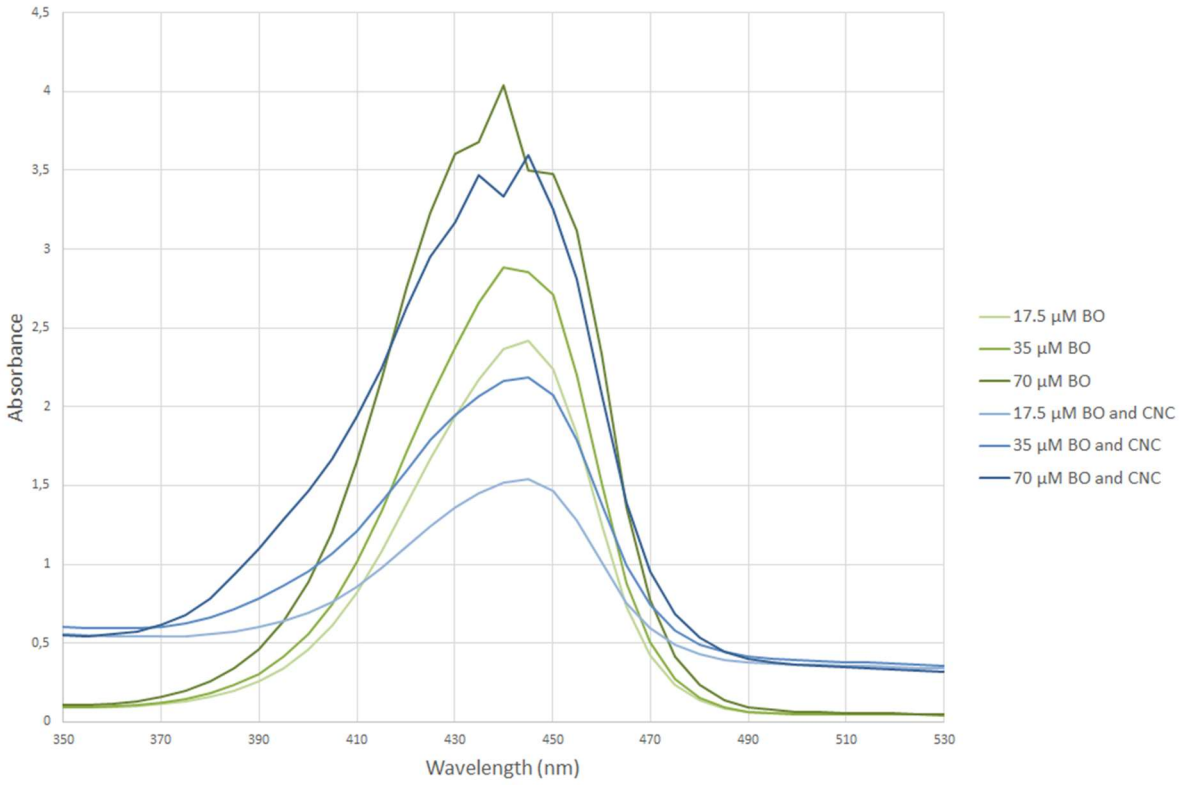

Figure 13. *Absorption spectra of different concentrations BO and 0.1 % CNC. All samples contained 25 mM of disodium phosphate buffer.*

As opposed to TO, BO does not show any indication of formation of aggregates upon addition of CNC (Figure 13). Neither does it seem to form any dimers with itself, as no peak shifts are observed at all. This is likely due to BO being too polar, as suggested in chapter 4.2.1 the aggregation of TO is likely promoted by its hydrophobicity, and studying the molecular structures of TO and BO (Figure 6 and 7) reveals that BO is definitely less hydrophobic than TO. It is possible however that BO might form aggregates with CNC or itself at other proportions not measured in this study.

4.3 Transfer of Cyanine Dye from CNC to DNA

At the wavelengths measured neither CNC and DNA nor the cyanines TO and BO showed any fluorescence of themselves. The CNC-Cyanine aggregates as well as the CNC-DNA mixture showed only little fluorescence (Figure 14 and 15). The DNA-Cyanine mixture however exhibited intense fluorescence, a strong indication that the cyanine intercalates with DNA.

In order to test if the cyanines TO and BO will release from the CNC surface and intercalate with DNA, different addition orders were performed on the samples subjected to spectroscopy analysis (Figure 14 and 15). DNA addition to the CNC-cyanine aggregates with low fluorescence made the samples fluoresce intensively, the same thing occurred upon cyanine addition to a CNC and DNA mixture. Whereas CNC addition to the already fluorescing DNA and TO mixture caused no substantial difference in fluorescence.

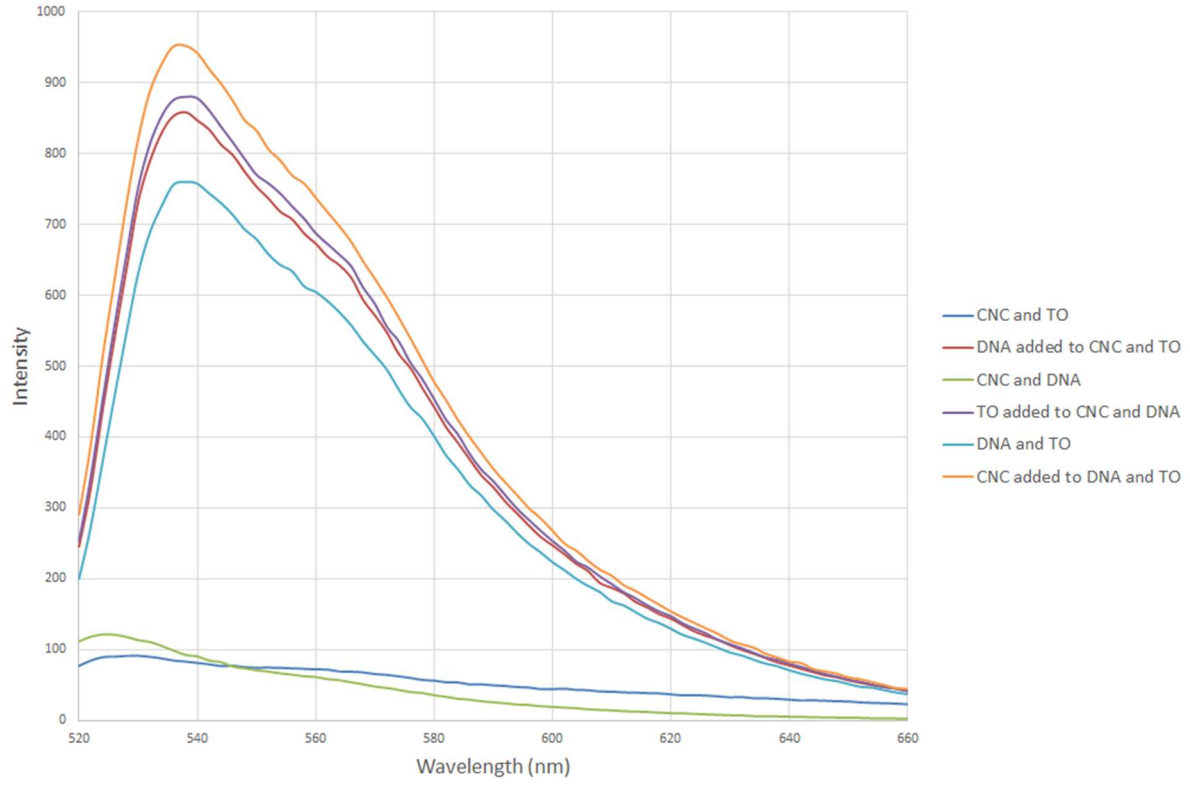

Figure 14. *Emission spectra of 0.05 % CNC, 35 µM TO and 100 µM DNA with varying addition orders, excited at 500 nm. All samples contained 25 mM of disodium phosphate buffer.*

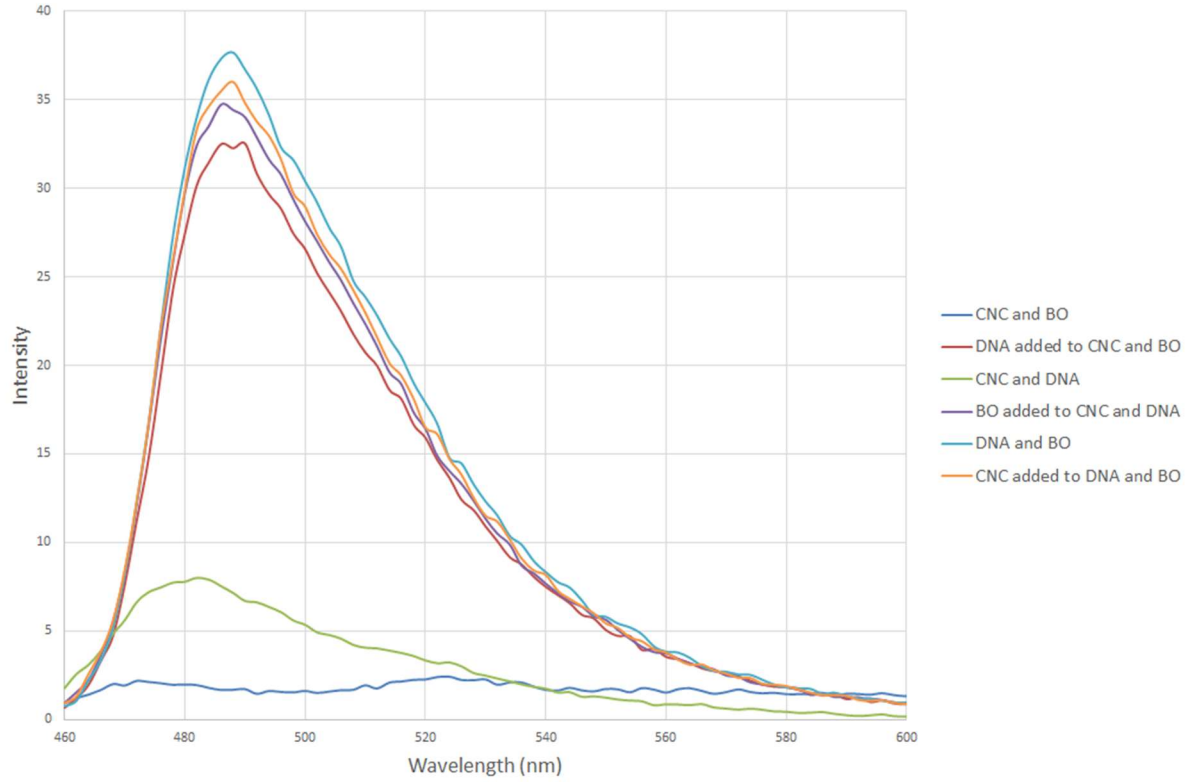

Figure 15. *Emission spectra of 0.05 % CNC, 35 µM BO and 100 µM DNA with varying addition orders, excited at 440 nm. All samples contained 25 mM of disodium phosphate buffer.*

To further show that the cyanines indeed disintegrate from CNC in favor to binding to DNA, the samples were subjected to absorption spectroscopy (Figure 16 and 17). In the absorption spectra for TO (Figure 16) a clear H-aggregate between CNC and TO can be seen at 440 nm, upon addition of DNA the peak of the H-aggregate disappears and the peak shift to 500 nm instead, the same wavelength as the suspected monomer of the cyanine is located. In the case for BO (Figure 17) there is no obvious H-aggregate, there is however a peak at 440 nm that is slightly displaced to 450 nm when DNA is added, indicating that BO might to a minor extent form some type of aggregate with itself. Interestingly this behavior could not be shown in chapter 4.2.2 (Figure 13) where the aggregation of BO was examined.

These results suggest that the cyanines TO and BO disintegrate from their CNC aggregates in favour of binding to DNA. The results were clearer for TO than BO since TO formed a well-defined H-aggregate, while BO only showed a slight sign of aggregation. However results from chapter 4.4 suggests that both cyanines TO and BO is attached to the CNC since they are close enough to quench the fluorescence of the sulfate groups on CNC.

It should also be noted that the difference in heights of the emission peaks in the 750 – 950 intensity area for TO (Figure 14) and 30-40 for BO (Figure 15) are not reliable readings. Samples with the same conditions were analyzed at a different day with freshly made solutions and did not give consistent results. The difference in intensity might be caused by rapid degradation or precipitation of the cyanine dyes or high sensitivity to inaccuracy when preparing these samples.

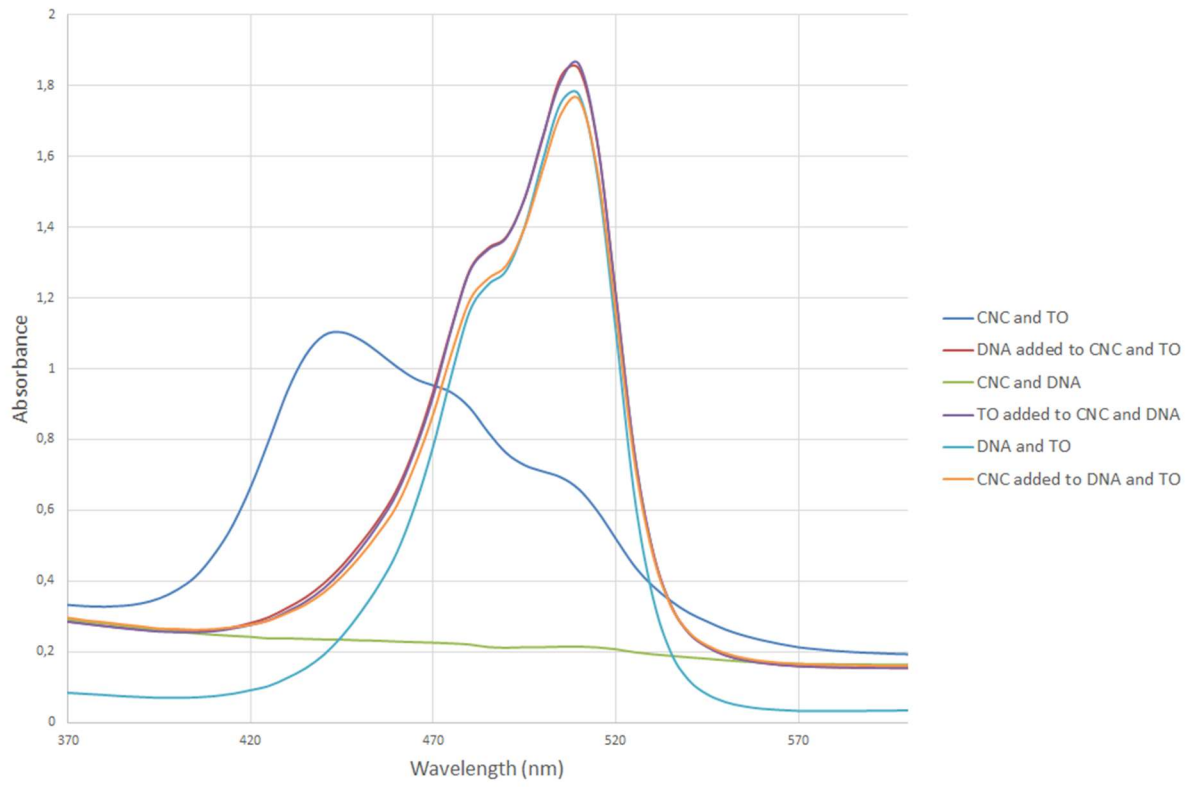

Figure 16. *Absorption spectra of 0.05 % CNC, 35 µM TO and 100 µM DNA with varying addition orders. All samples contained 25 mM of disodium phosphate buffer.*

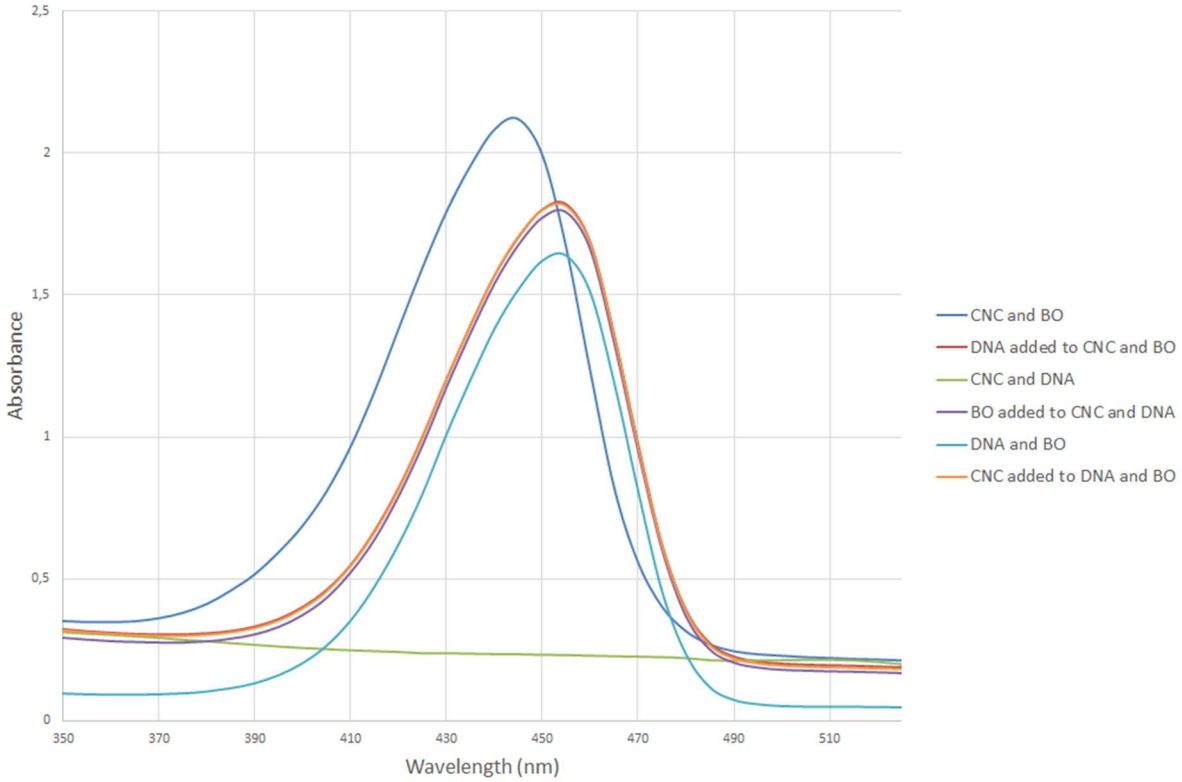

Figure 17. *Absorption spectra of 0.05 % CNC, 35 µM BO and 100 µM DNA with varying addition orders. All samples contained 25 mM of disodium phosphate buffer.*

4.4 Quantification of sulfate groups on CNC

To evaluate if addition of cyanines to CNC can potentially be used to quantify the amount of sulfate groups on CNC, samples containing CNC and varying concentrations of the cyanine dyes TO and BO were subjected to emission spectroscopy at 290 nm.

The results showed (Figure 18 and 19) that addtion of TO and BO caused the fluorescence of the sulfate groups on CNC to decrease. The two cyanines did not reduce the fluorescence in the exact same manner, for TO the difference in fluorescence caused between the 35 and 70 µM TO were roughly the same as for the difference between 17.5 and 35 µM TO, even though the difference in concentration is twice as much between 35 and 70 µM than between 17.5 and 35 µM. While for BO the difference in peak intensities seem to follow the differences in BO concentrations in a more linear way .

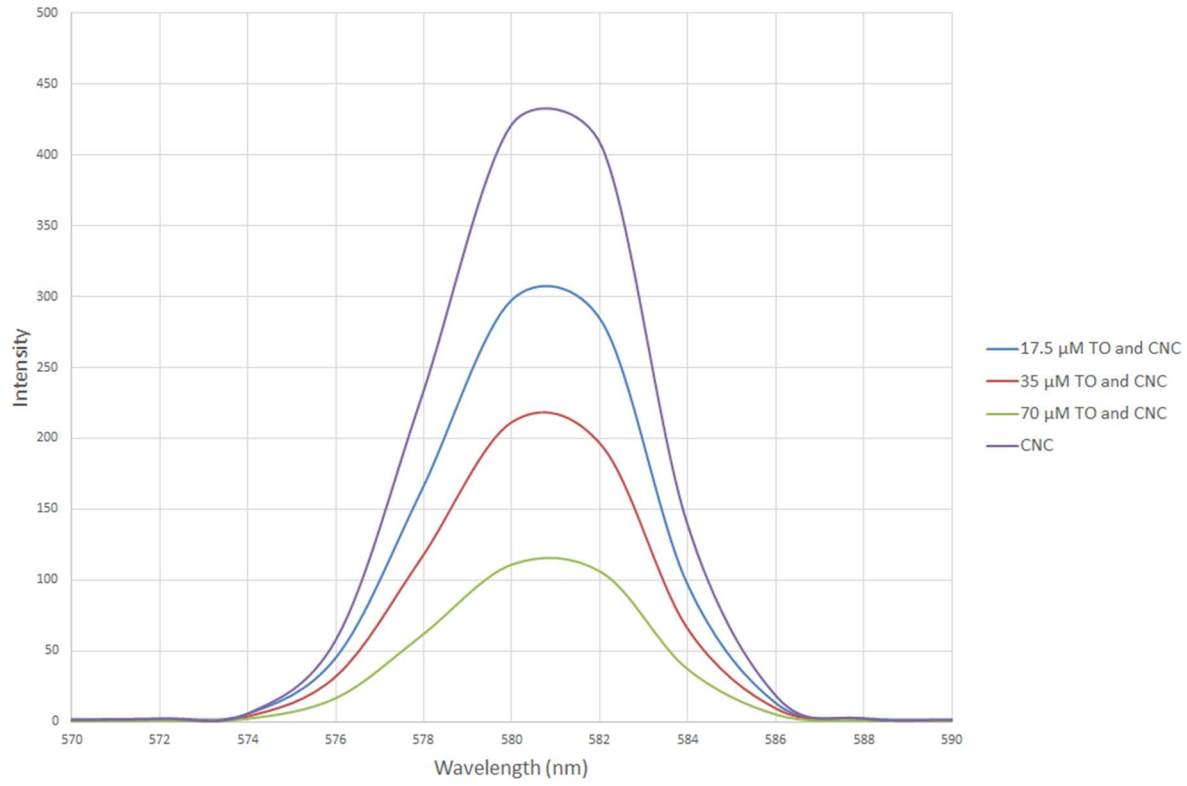

Figure 18. *Emission spectra of different concentrations TO and 0.1 % CNC, excited at 290 nm. All samples contained 25 mM of disodium phosphate buffer.*

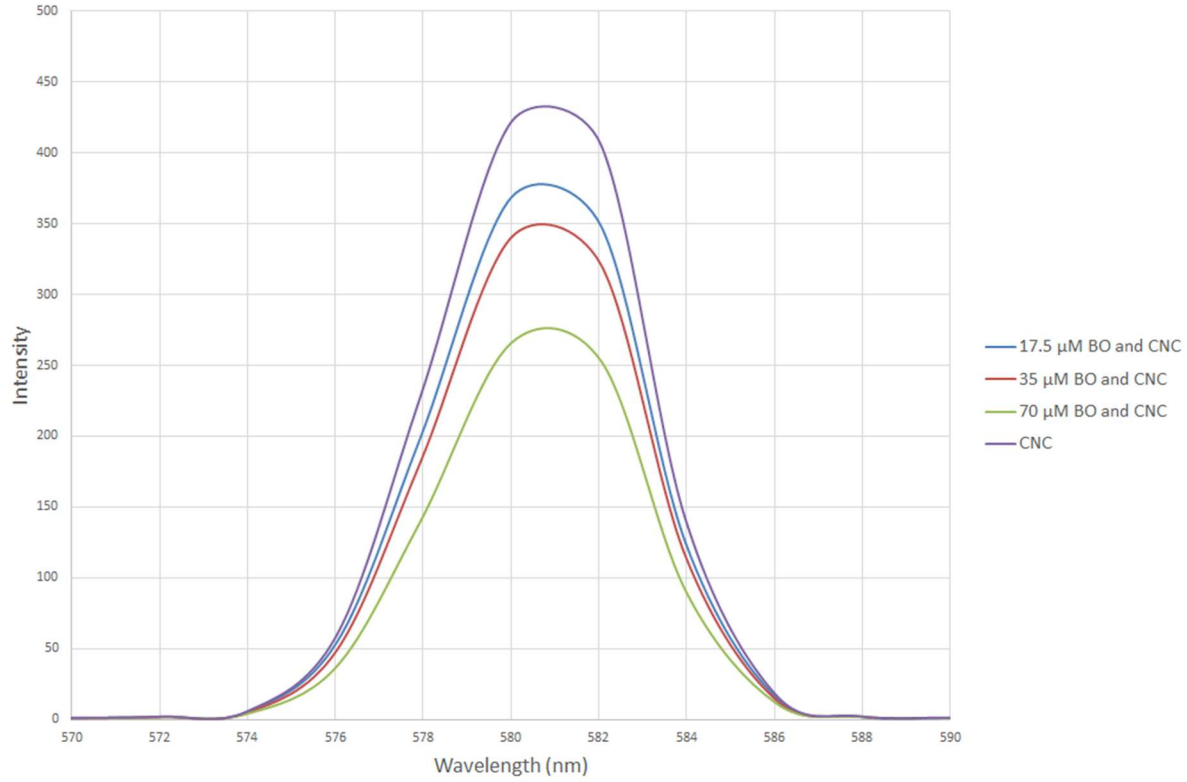

Figure 19. *Emission spectra of different concentrations BO and 0.1 % CNC, excited at 290 nm. All samples contained 25 mM of disodium phosphate buffer.*

The method of quantifying sulfonate groups on CNC using the cyanine dyes TO and BO looks promising. In order to further develop this method more testing must be conducted, such as analysing multiple samples with cyanine together with polysulfonate standards with known quantity of sulfonate groups. This data would be necessary when using this method as a reliable method for quantification of sulfonate groups on CNC.

In order to examine if the fluorescence of non-polymeric sulfonate groups can be quantified in the same manner, samples of sodium p-toluenesulfonate were mixed with different concentrations of TO and BO and analyzed in the same way as the CNC was. The results (Appendix 1 and 2) showed that these sulfonate groups did not behave as those in CNC. For instance 17.5 and 35 µM TO quenched the fluorescence of the sulfonate the same amount, and addition of 17.5 µM BO surprisingly caused a greater fluorescence than the sulfate group itself. These results suggest that this method is probably not viable for quantification of non-polymeric sulfonate groups.

The same analyses were also performed on the structurally simpler aromatic amines pyridine and 1,4-Dimethylpyridinium p-toluenesulfonate in order to see if they could quench the fluoerescence of the sulfonate groups on CNC just as the cyanines TO and BO could. The emission spectras (Appendix 3 and 4) showed that they did not reduce the fluoerescence of the sulfonate groups at all.

5. CONCLUSIONS

The results shows that TO forms dimers with itself and H-aggregates together with CNC, BO on the other hand did not show signs of aggregation with itself nor with CNC at the measured concentrations.

It was also shown that both TO and BO can be transferred from CNC to DNA in aqueous solutions, TO and BO performed equally well in these transfers. The results confirm that CNC can be used as a drug carrier for cyanine dyes to DNA in vitro.

The examination of using the TO and BO in quantification of sulfate groups on CNC concluded that it should be possible to use these cyanine dyes to further develop a quantification method for sulfate groups on polysulfonates.

6. ACKNOWLEDGEMENTS

I would like to thank the following people who have helped me with this project:

Gunnar Westman, supervisor and project leader for his valuable advice and guidance throughout the project.

Karin Sahlin for advice and help with spectroscopy analysis.

Erik Edsinger for assistance with cyanine dye synthesis as well as spectroscopy analysis.

Anders Mårtensson for performing AFM analysis.

REFERENCES

[1] Kawakami M, Koya K, Tatsuta T, Noriaki UT, Ikegawa A, Ogawa K, et al. Structure-activity of novel rhodacyanine dyes as antitumor agents. Journal of Medicinal Chemistry. 1998;41(1):130-42.

[2] Biver T, García B, Leal JM, Secco F, Turriani E. Left-handed DNA: Intercalation of the cyanine thiazole orange and structural changes. A kinetic and thermodynamic approach. Physical Chemistry Chemical Physics. 2010;12(40):13309-17.

[3] Karlsson HJ, Bergqvist MH, Lincoln P, Westman G. Syntheses and DNA-binding studies of a series of unsymmetrical cyanine dyes: structural influence on the degree of minor groove binding to natural DNA. Bioorganic & Medicinal Chemistry. 2004;12(9):2369-84.

[4] Chakraborty S, Debnath P, Dey D, Bhattacharjee D, Hussain S. Formation of fluorescent H-aggregates of a cyanine dye in ultrathin film and its effect on energy transfer. JOURNAL OF PHOTOCHEMISTRY AND PHOTOBIOLOGY A-CHEMISTRY. 2014;293:57-64.

[5] Šponar J, Votavová H. Selective binding of synthetic polypeptides to DNA of varying composition and sequence: Effect of minor groove binding drugs. Journal of Biomolecular Structure and Dynamics. 1996;13(6):979-89.

[6] Al-khouri S. UV/Vis and CD Spectral Studies of the Interaction between Pinacyanol Chloride and Alginates, γ-Cyclodextrin, and Aerosol-OT [dissertation]. Duisberg: University of Duisburg-Essen; 2003.

[7] De Jong WH, Borm PJA. Drug delivery and nanoparticles: Applications and hazards. International Journal of Nanomedicine. 2008;3(2):133-49.

[8] Peng BL, Dhar N, Liu HL, Tam KC. Chemistry and applications of nanocrystalline cellulose and its derivatives: A nanotechnology perspective. The Canadian Journal of Chemical Engineering. 2011;89(5):1191-206.

[9] Brinchi L, Cotana F, Fortunati E, Kenny JM. Production of nanocrystalline cellulose from lignocellulosic biomass: Technology and applications. Carbohydrate Polymers. 2013;94(1):154-69.

[10] Ehmann H, Mohan T, Koshanskaya M, Scheicher S, Breitwieser D, Ribitsch V, et al. Design of anticoagulant surfaces based on cellulose nanocrystals. CHEMICAL COMMUNICATIONS. 2014;50(86):13070-2.

[11] Mishra A, Behera RK, Behera PK, Mishra BK, Behera GB. Cyanines during the 1990s: a review. Chemical Reviews. 2000;100(6):1973-2011.

[12] Gadde S, Batchelor EK, Kaifer AE. Controlling the formation of cyanine dye H- and J-aggregates with cucurbituril hosts in the presence of anionic polyelectrolytes. Chemistry - A European Journal. 2009;15(24):6025-31.

[13] Marchetti AP, Salzberg CD, Walker EIP. The optical properties of crystalline 1,1′-diethyl-2,2′-cyanine iodide. The Journal of Chemical Physics. 1976;64(11):4693-8.

[14] Liu C, Lu Y, He S, Wang Q, Zhao L, Zeng X. The nature of the styrylindolium dye: transformations among its monomer, aggregates and water adducts. JOURNAL OF MATERIALS CHEMISTRY C. 2013;1(31):4770-8.

[15] Biver T, Boggioni A, Secco F, Turriani E, Venturini M, Yarmoluk S. Influence of cyanine dye structure on self-aggregation and interaction with nucleic acids: A kinetic approach to TO and BO binding. Archives of Biochemistry and Biophysics. 2007;465(1):90-100.

[16] Nada AMA, El-Kady MY, Abd El-Sayed ES, Amine FM. Preparation and characterization of microcrystalline cellulose (MCC). BioResources. 2009;4(4):1359-71.

[17] Segal L, Creely JJ, Martin AE, Conrad CM. An Empirical Method for Estimating the Degree of Crystallinity of Native Cellulose Using the X-Ray Diffractometer. Textile Research Journal. 1959;29(10):786-94.

[18] Park S, Baker JO, Himmel ME, Parilla PA, Johnson DK. Cellulose crystallinity index: Measurement techniques and their impact on interpreting cellulase performance. Biotechnology for Biofuels. 2010;3(1):1-10.

[19] Huq T, Salmieri S, Khan A, Khan RA, Le Tien C, Riedl B, et al. Nanocrystalline cellulose (NCC) reinforced alginate based biodegradable nanocomposite film. Carbohydrate Polymers. 2012;90(4):1757-63.

[20] Wang N, Ding E, Cheng R. Surface modification of cellulose nanocrystals. Frontiers of Chemical Engineering in China. 2007;1(3):228-32.

APPENDIX

Quantification of sulfate groups on CNC

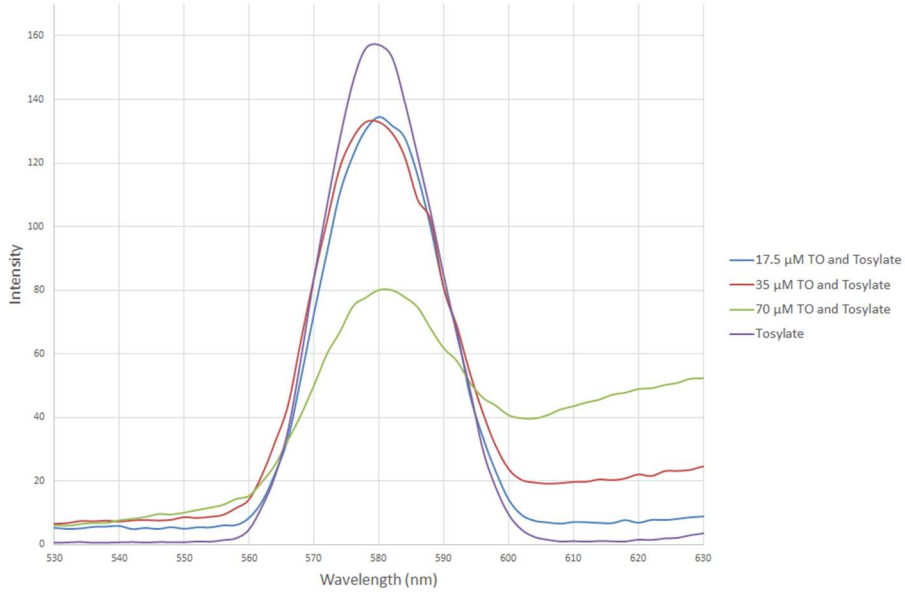

Appendix 1. *Emission spectra of different concentrations TO and 70 µM* sodium tosylate*, excited at 290 nm. All samples contained 25 mM of disodium phosphate buffer.*

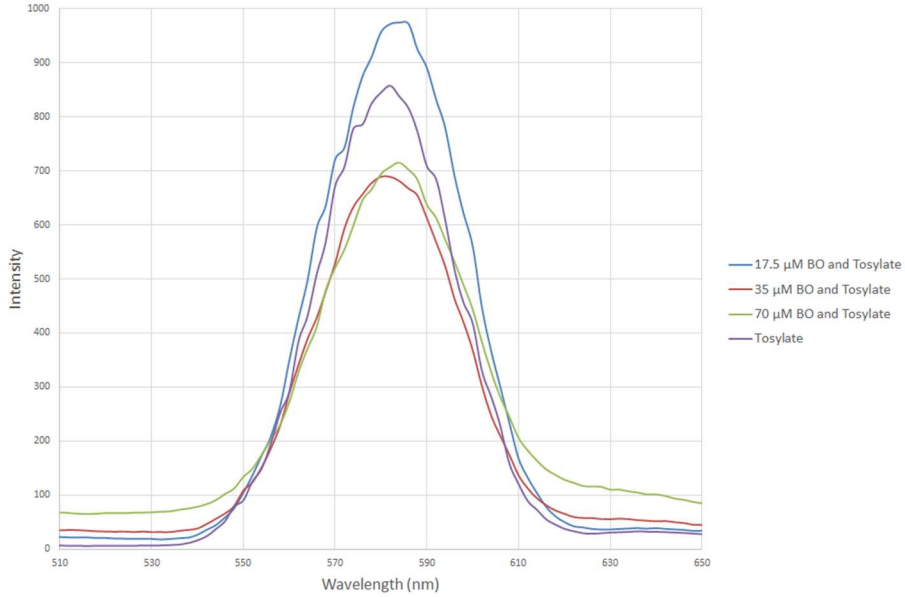

Appendix 2. *Emission spectra of different concentrations BO and 70 µM* sodium tosylate*, excited at 290 nm. All samples contained 25 mM of disodium phosphate buffer.*

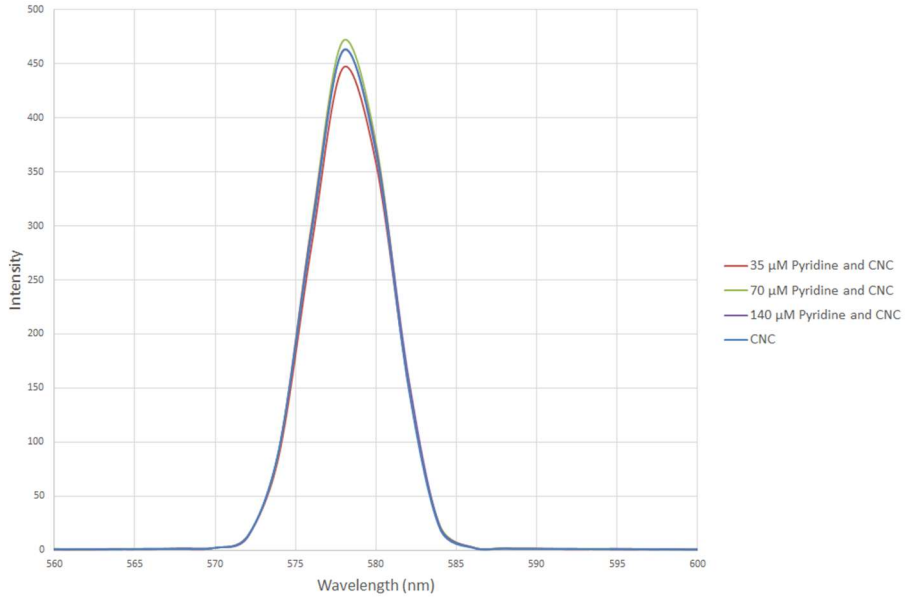

Appendix 3. *Emission spectra of different concentrations pyridine and 0.1 % CNC, excited at 290 nm. All samples contained 25 mM of disodium phosphate buffer.*

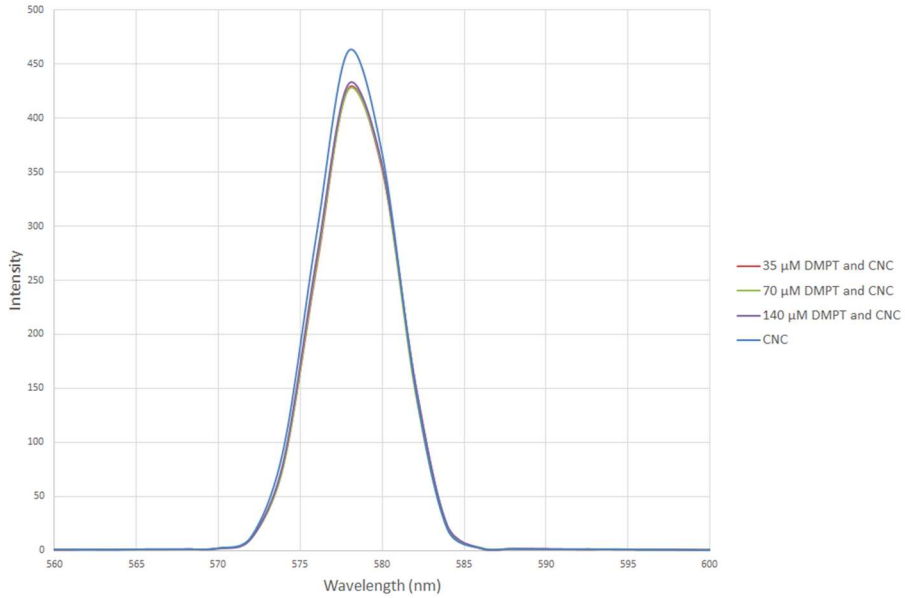

Appendix 4. *Emission spectra of different concentrations 1,4-Dimethylpyridinium p-toluenesulfonate (DMPT) and 0.1 % CNC, excited at 290 nm. All samples contained 25 mM of disodium phosphate buffer*